The Fermi surface of UPd_2Al_3

1996 J. Phys.: Condens. Matter 8 901

(http://iopscience.iop.org/0953-8984/8/7/014)

J. Phys.: Condens. Matter **8** (1996) 901–909. Printed in the UK

The Fermi surface of UPd_2Al_3

K Knöpfle, A Mavromaras, L M Sandratskii and J Kübler
Institut für Festkörperphysik, Technische Hochschule, D-64289 Darmstadt, Germany

Received 28 September 1995

Abstract. The de Haas–van Alphen spectrum of UPd_2Al_3 is calculated and compared with the experimental spectrum for continuously varying directions of the magnetic field. The local density approximation to spin-density functional theory is used for the self-consistent calculations treating the U 5f electrons as itinerant and including spin–orbit coupling. The amount of f angular momentum character is obtained and exhibited graphically for each sheet of the Fermi surface. The band-decomposed spin susceptibility, χ_0, is calculated for the states at the Fermi surface and the anisotropy of χ_0 is discussed.

1. Introduction

The discovery [1] of the coexistence of superconductivity and antiferromagnetism in the heavy-fermion compound UPd_2Al_3 has generated great interest in its electronic structure. This was consequently calculated in the local spin-density functional approximation (LSDA) in attempts to understand the physics of this compound [2, 3]. Thus the magnetic properties and the topology of the Fermi surface together with a number of de Haas–van Alphen (dHvA) frequencies, which were calculated for two magnetic field directions chosen parallel and perpendicular to the hexagonal z axis, were the centre of attention in [3]. These selected dHvA frequencies were found to be in good agreement with experimental data. We emphasize that in these calculations—and those that follow—all U 5f electrons were assumed to be itinerant, hybridizing with the conduction electrons of U, Pd and Al. Since the Fermi surface is found to be predominantly determined by the U 5f electrons, the agreement with experiment is significant for the ongoing discussion concerning the treatment of 5f electrons, itinerant or localized.

In the present paper we complete the Fermi surface studies of UPd_2Al_3 by focusing our attention on essentially two different aspects. First, the entire spectrum of dHvA frequencies is calculated for continuously varying directions of the magnetic field; this enables us to make an extremely detailed comparison of the theoretical and experimental data. Second, we determine and visualize the angular momentum character and the degree of hybridization of the electron states from different sheets of the Fermi surface as well as different parts of the same sheet. With these calculations we address the question as to whether or not in the itinerant-electron description there can be two different groups of uranium 5f states in UPd_2Al_3. This question was raised by Steglich *et al* in recent experimental work [4, 5, 6], the analysis of which quite plausibly requires such an assumption. In particular one group of 5f states is supposed to be rather localized and responsible for the magnetic properties whereas the other is less localized and responsible for the superconducting properties of the compound. Furthermore, they are distinguished by different anisotropies in the spin susceptibilities which we also estimate. Although our results cannot definitely prove the

0953-8984/96/070901+09$19.50

validity of this assumption in detail, they nevertheless lend weight to the general point of view.

2. Calculational approach

The experimentally determined crystal structure, lattice constant and c/a ratio as described before [3] as well as the experimentally observed antiferromagnetic ground state [1, 7] sketched in figure 1 were used in our calculations which were carried out in the LSDA employing the relativistic version described in [3] of the ASW method [8]. Thus our calculations incorporate the spin–orbit interaction which is large for uranium. To visualize the difference between the electronic states on the Fermi surface we use colour prints showing the 5f contribution to every state. The continuous colour scale reflects the size of the 5f contribution ranging from zero to 100%. The graphics shown was produced by using the IBM product 'Data Explorer'.

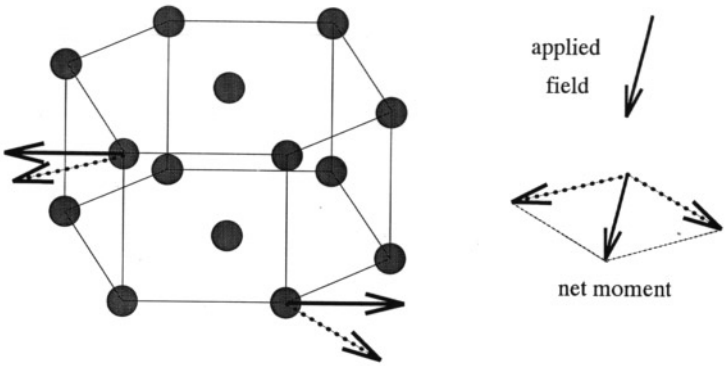

Figure 1. The crystal structure of UPd_2Al_3 and the magnetic order. Only the uranium atoms are shown.

To obtain additional information on the character of the electron states at the Fermi level, E_F, we estimate the anisotropy of the magnetic susceptibility of the different bands at E_F. To do this, we calculate the electronic response by applying a magnetic field, i.e. by adding the Zeeman term

$$H_B = \mu_B \boldsymbol{B} \cdot (\boldsymbol{l} + 2\boldsymbol{s}) \tag{1}$$

to the Kohn–Sham Hamiltonian. Here $\boldsymbol{B}$ is the applied magnetic field, and $\boldsymbol{l}$ and $\boldsymbol{s}$ are, respectively, the operators of the orbital and spin angular momentum. The *unenhanced* response is obtained as in earlier work [9]; in a first step the self-consistent calculation is performed without an applied field, and then one iteration is carried out with the field applied. The magnetic moment is obtained separately for each band and, dividing by the applied field, we obtain a band-decomposed magnetic susceptibility. Calculations are done for two directions of the magnetic field—parallel to the y axis and parallel to the z axis. Because in both cases the field is perpendicular to the initial directions of the magnetic moments the canting of the magnetic moments toward the direction of the field, see figure 1, is taken into account by allowing noncollinear configurations of the magnetic moments [10].

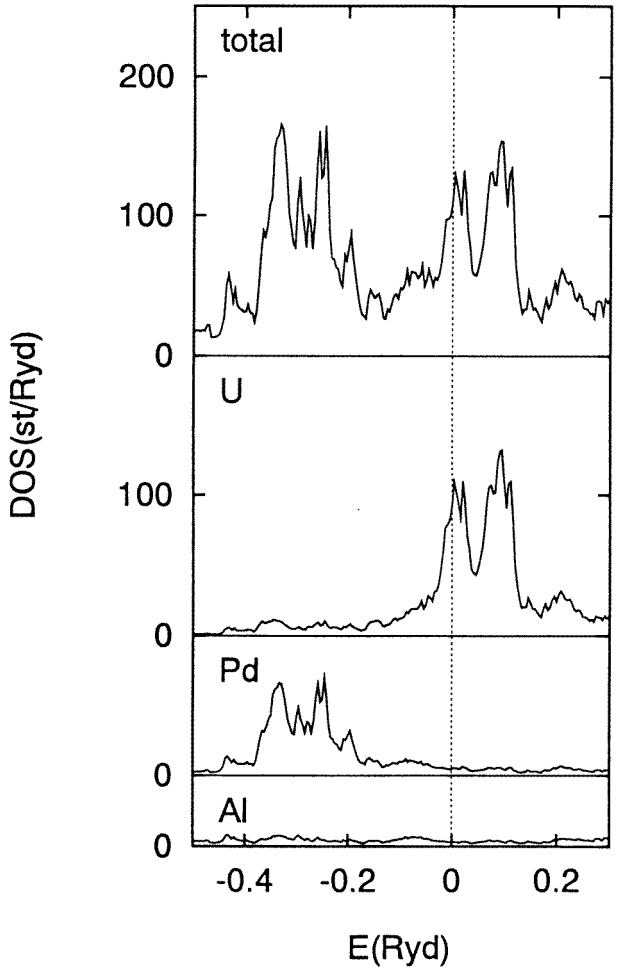

Figure 2. Total and partial densities of states.

3. Results and discussion

To convey a general impression of the electronic structure of UPd_2Al_3 we first show in figure 2 the total and partial densities of states (DOS) of the compound in the ground state. In figure 3 the energy distribution curves measured in photoemission experiments [11] and assigned, respectively, to U 5f and Pd states are compared with the corresponding partial DOS from figure 2. Concerning the Pd states, it is seen that the photoemission intensities agree nicely with the calculated partial Pd DOS. This is different for the U 5f states; although both curves indicate the presence of 5f states at and near the Fermi level, they, nevertheless, have quite different shapes. This should, however, not be surprising since these curves must not be compared without caution. We refer the reader to a discussion in [11] of the limitations of LSDA theory in describing photoemission spectra of U 5f electrons.

We now turn to the main topic, the Fermi surface (FS), but before engaging in a detailed discussion we point out the difference of the present results from those of [3]. There the FSs

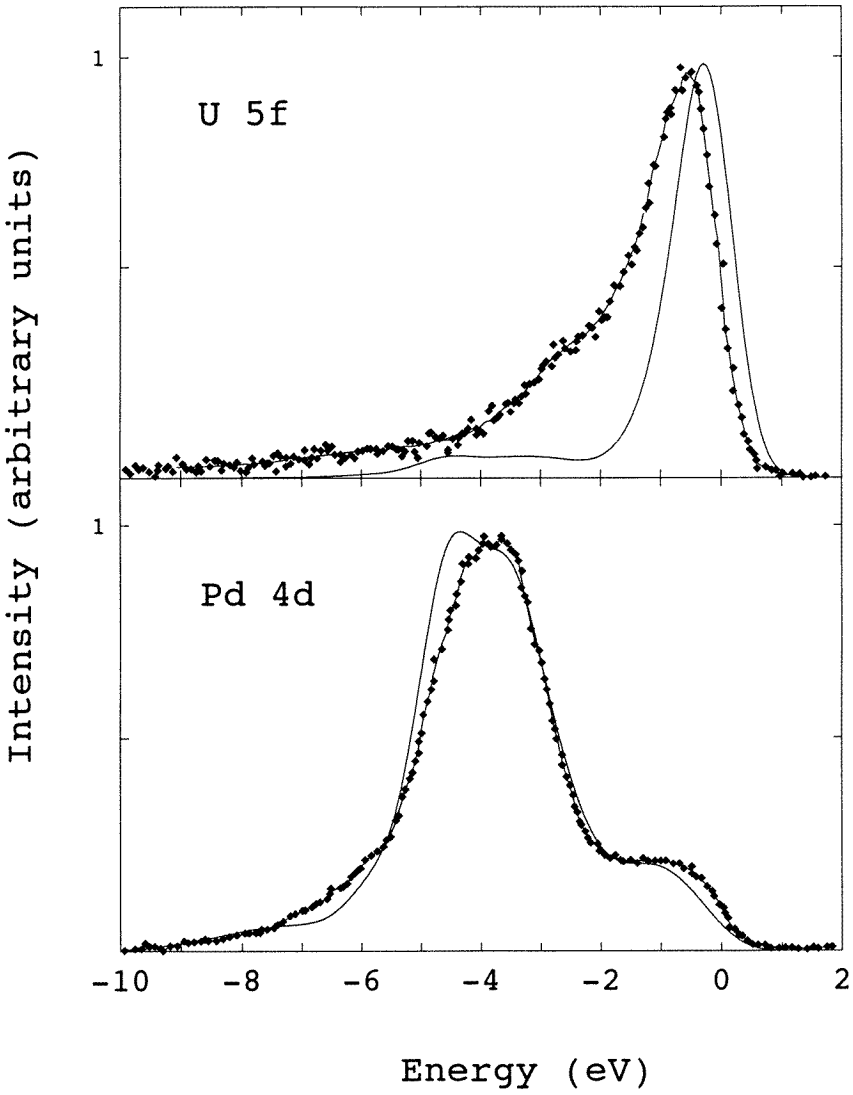

Figure 3. A comparison of experimental photoemission intensities [11] with calculated partial densities of states.

displayed possess the full symmetry of the hexagonal lattice. This is an approximation since the magnetic order reduces the symmetry to orthorhombic. The data shown here possess orthorhombic symmetry as they should, but the differences of the present data from those obtained earlier are small.

Our new results are shown in figure 4 where the experimental [12, 13] and the calculated dHvA frequencies are given as functions of the direction of the magnetic field. The labelling of the various frequency branches corresponds to the extremal cross sections that are defined in figure 5. The agreement of the calculated and the experimental data is in general good but varies from FS sheet to FS sheet. Thus, for both parts of the second sheet of the FS, figure 5(b), we obtain very good agreement—see the α-, β- and γ-frequencies in figure 4.

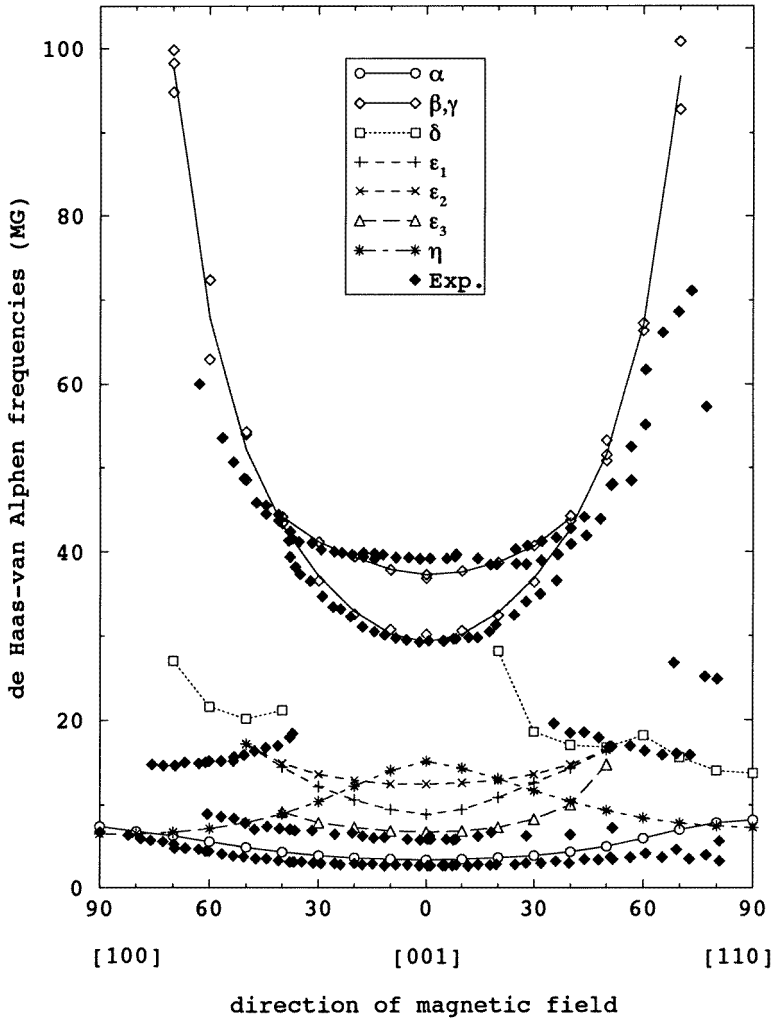

Figure 4. Experimental [12, 13] and calculated de Haas–van Alphen frequencies as functions of the angle of the applied magnetic field with respect to the *c* axis.

For the rather complicated first sheet of the FS, figure 5(a), we find four different extremal cross sections: ε_1, ε_2, ε_3, and δ. Unfortunately, the experimental data are not so rich. Still we can identify one of the ε cross sections and the γ cross section although the latter is not as symmetric as the experimental one with respect to the origin in figure 4. But no counterparts for two other ε cross sections are detected experimentally; neither is the η cross section of the third sheet observed (see figure 5(c)). Thus, except for some scattered frequencies, we find a theoretical partner for the observed experimental extremal cross sections; however, the calculation supplies some extremal cross sections that are not detected experimentally. This might be due to the fact that the amplitude of each oscillation depends on the local curvature of the Fermi surface round the extremal cross section [14].

We next turn to an analysis of the angular momentum character of the states forming various sheets of the FS. Here the important quantity, no doubt, is the amount of U 5f

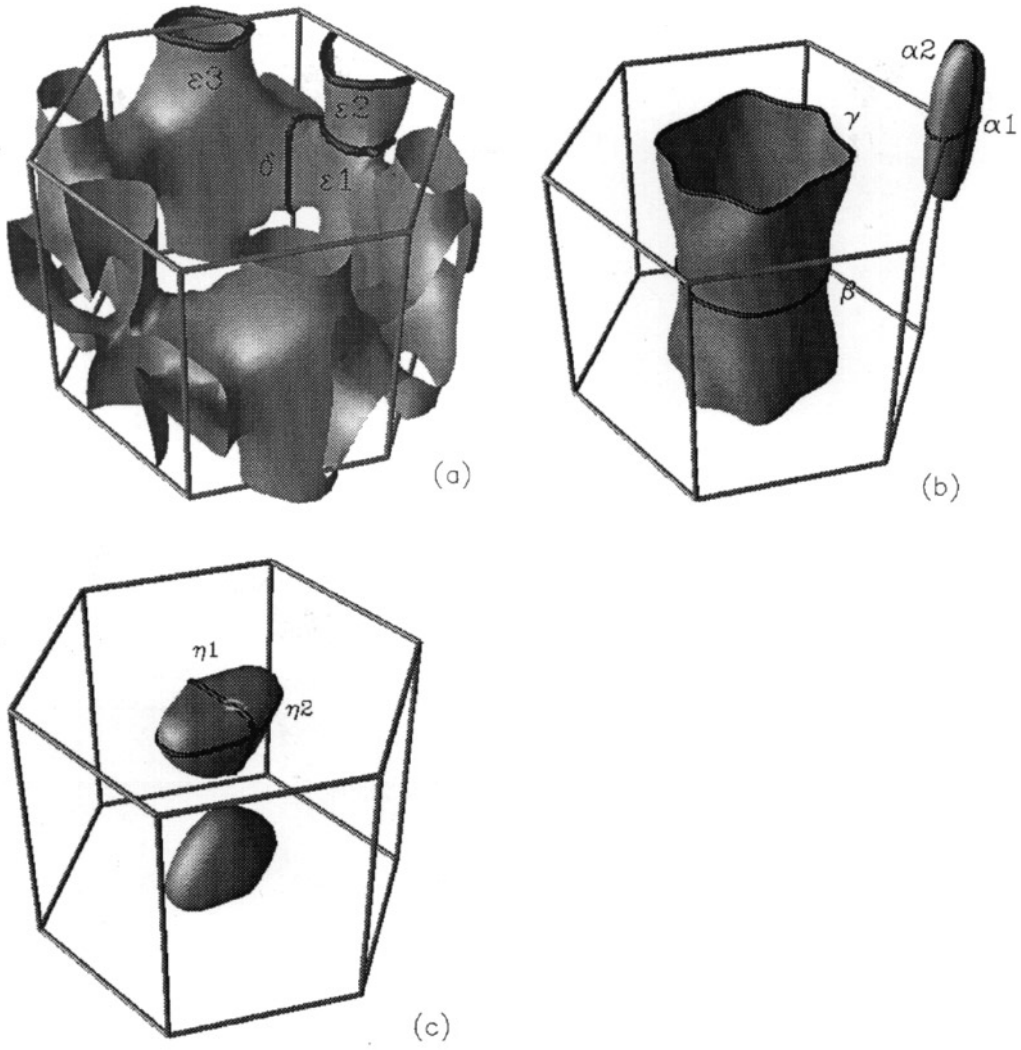

Figure 5. Definitions of the various extremal orbits employed in figure 4: (a) the 'party hat'; (b) the 'column' and 'cigars'; (c) the 'egg'.

character which is the 5f-and-U-site-decomposed density of states for each point in k-space on the Fermi surface. This parameter is displayed in colour-graphics form in figure 6 where the fractional contribution of the U 5f states is represented by different colours according to the scale diagram shown in figure 6. The broad variation of the colour from blue to red reflects a substantial variation of the 5f contribution for different groups of states which change in the range from about 25% to about 90%. However, this distribution is different for different parts of the Fermi surface. Thus the entire 'column' part of the second sheet of the FS is formed by almost pure U 5f states. The second smaller 'cigar' part of the same sheet contains states with a much smaller 5f contribution of about 50% only. The third, 'egg' sheet has an intermediate contribution of 5f states of around 75%. Finally, the first sheet, which could be called the 'party hat', contains very different states in different parts

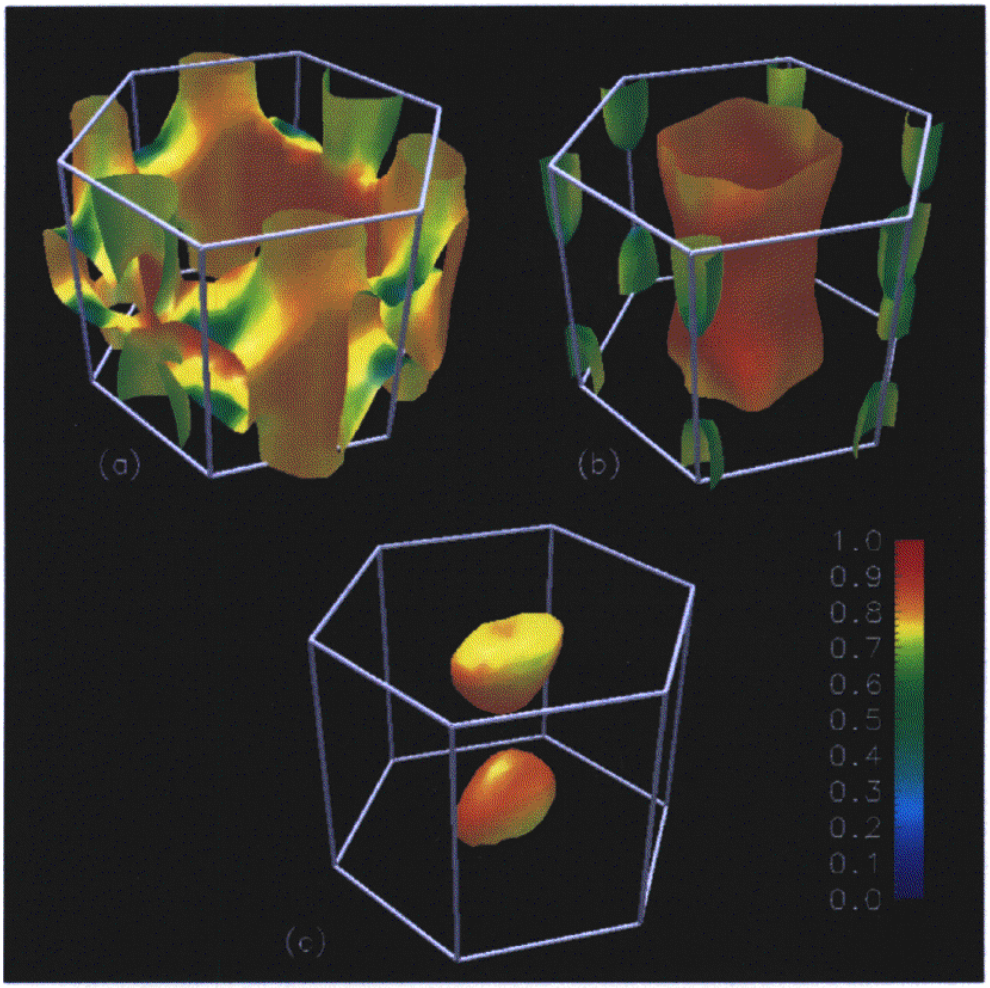

Figure 6. Fermi surfaces as in figure 5. The colours shown give the amount of 5f angular momentum character on each sheet of the Fermi surface.

of the surface. We stress the distinction of the two largest sheets of the FS: 'party hat' and 'column'. The latter is an almost pure 5f sheet in contrast to the former which is formed by strongly hybridized states. Again, the extent of the hybridization is very different in different parts of the surface.

This result lends considerable weight to the assumption about different types of state at the Fermi level made in [4, 5, 6]. Since one of the experimental distinctions is the anisotropy of the magnetic susceptibility we extend the comparison by calculating the magnetic response of the bands forming different sheets of the FS to a magnetic field applied, respectively, parallel to the y and the z axes (figure 1) as described in the previous section. The value of the field is chosen so that $\mu_B B$ equals 1 mRyd. The results of the calculation of the susceptibility are collected together in table 1. Note that in the absence of the field the collinear antiferromagnetic structure leads to double degeneracy of all energy bands and therefore of all sheets of the FS. The external magnetic field lowers the symmetry and lifts the degeneracy of the bands. As a result, the two degenerate bands

respond differently to the applied field. From table 1 we see that band 3 ('eggs') gives a relatively small value of the magnetic susceptibility. Comparison of bands 1 with bands 2 ('party hat' with 'column') shows a much stronger anisotropy of the susceptibility of the sub-bands in the case of band 2, i.e. the 'columns'. This is again in parallel with the observation of [4, 5, 6].

Table 1. Magnetic susceptibility of different bands in μ_B mRyd^{-1}, with a magnetic field of 1 mRyd in the z and y directions.

Fermi surface	χ_z	χ_y
1a 'party hat'	0.204	0.243
1b 'party hat'	−0.132	−0.183
2a 'column and cigars'	0.126	0.059
2b 'column and cigars'	−0.074	−0.019
3a 'egg'	0.012	0.019
3b 'egg'	−0.013	−0.007

4. Conclusion

The good agreement of the theoretical and the experimental data for the photoemission and the dHvA experiments found here, and the magnetic properties studied in an earlier publication [3] strongly support the itinerant-electron picture for UPd_2Al_3. However, the observed heavy masses cannot be obtained within the local spin-density functional approximation; see [15] for a possible explanation. The study of the 5f contribution to the states forming the Fermi surface (FS) shows that it differs markedly for different groups of the electron states. We contrast the two largest sheets of the FS, the 'column' with the 'party hat' (figure 6). The former contains almost pure 5f states whereas the latter contains strongly hybridized states with the 5f contribution decreasing to as low a value as 30%. The study of the anisotropy of the magnetic susceptibility for the corresponding two energy bands also shows a substantial difference, being rather isotropic for the bands forming the 'party hat' and strongly anisotropic for the bands forming the 'column'. We interpret the difference between the properties of the two Fermi surfaces as supporting the assumption about two different types of the 5f electron in UPd_2Al_3 made in [4, 5, 6] on the basis of experimental data.

Acknowledgments

We are indebted to I Mertig and P Zahn for a number of helpful discussions. This work was supported by the SFB 252 Darmstadt, Frankfurt, Mainz. It also benefited from collaboration within the European Union's Human Capital and Mobility Network on 'Ab initio (from electronic structure) calculation of complex processes in materials' (contract: ERBCHRXCT930369)

References

[1] Geibel C, Böhm A, Caspary R, Gloos K, Grauel A, Hellmann P, Modler R, Schank C, Weber G and Steglich F 1993 *Physica* B **186–188** 188

[2] Sticht J and Kübler J 1992 *Z. Phys.* B **87** 299

[3] Sandratskii L M, Kübler J, Zahn P and Mertig I 1994 *Phys. Rev.* B **50** 15 834
[4] Caspary R, Hellmann P, Keller M, Sparn G, Wassiliew C, Köhler R, Geibel C, Schank C, Steglich F and Phillips N E 1993 *Phys. Rev. Lett.* **71** 2146
[5] Feyerherm R, Amato A, Gygax F N, Schenk A, Geibel C, Steglich F, Sato N and Komatsubara T 1994 *Phys. Rev. Lett.* **73** 1849
[6] Steglich F, Buschinger B, Gegenwart P, Geibel C, Helfrich R, Hellmann P, Lang M, Link A, Modler R, Jaccard D and Link P 1996 *Int. J. Mod. Phys.* at press
[7] Paolasini J, Paixao J A, Lander G H, Burlet P, Sato N and Komatsubara T 1994 *Phys. Rev.* B **49** 7072
[8] Williams A R, Kübler J and Gelatt C D 1979 *Phys. Rev.* B **19** 6094
[9] Sandratskii L M and Kübler J 1992 *J. Phys.: Condens. Matter* **4** 6927
[10] Sticht J, Höck K H and Kübler J 1989 *J. Phys.: Condens. Matter* **1** 8155
[11] Ejima T, Suzuki S, Sato S, Sato N, Fujimori S, Yamada M, Sato K, Komatsubara T, Kasuya T, Tezuka Y, Shin S and Ishii T 1994 *J. Phys. Soc. Japan* **63** 2428
[12] Inada Y, Aono H, Ishigura A, Kimura J, Sato N, Sawada A and Komatsubara T 1994 *Physica* B **189–200** 119
[13] Inada Y, Ishigura A, Kimura J, Sato N, Sawada A, Komatsubara T and Yamagami H 1995 *Physica* B **206–207** 33
[14] Ziman J M 1969 *Principles of the Theory of Solids* (Cambridge: Cambridge University Press) p 279
[15] Steiner M M, Albers R C and Sham L J 1994 *Phys. Rev. Lett.* **72** 2923